Article ID: 1000-7032(2013)06-0732-06

Temperature-dependent Upconversion Luminescence of β-$NaYF_4$: Yb^{3+}, Er^{3+} Nanoplates

ZHAO Jun-wei[1,2*], WANG Xiao-feng[2],
WANG Yu-jiang[2], ZENG Qing-hui[1], KONG Xiang-gui[1*]

(1. *State Key Laboratory of Luminescence and Applications, Changchun Institute of Optics, Fine Mechanics and Physics, Chinese Academy of Sciences, Changchun* 130033, *China*;
2. *Department of Materials Science and Engineering, Luoyang Institute of Science and Technology, Luoyang* 471023, *China*)
* *Corresponding Author, E-mail: jwzhao*168@*yahoo. com. cn; xgkong*14@*ciomp. ac. cn*

Abstract: Temperature dependent characteristics of upconversion luminescence in β-$NaYF_4$: Yb^{3+}, Er^{3+} nanoplates under 980 nm excitation were reported. Intense green and red upconversion emissions corresponding to ($^2H_{11/2}$, $^4S_{3/2}$) → $^4I_{15/2}$ and $^4F_{9/2}$ → $^4I_{15/2}$ transitions of the Er^{3+} ions were observed, respectively. The green emission around 520 nm and the red emission around 660 nm continuously increase with increasing of temperature. The emission around 545 nm increases from 84 to 204 K and then decreases from 204 to 483 K. The temperature dependence of intensity characteristics was systematically analyzed by a simple three-level system.

Key words: upconversion; β-$NaYF_4$; rare earth; temperature-dependent; three-level system
CLC number: O482.31 **Document code**: A **DOI**: 10.3788/fgxb20133406.0732

温度依赖的 β-$NaYF_4$: Yb^{3+}, Er^{3+} 纳米片的上转换发光

赵军伟[1,2*], 王晓峰[2], 王玉江[2], 曾庆辉[1], 孔祥贵[1*]

(1. 发光学及应用国家重点实验室 中国科学院长春光学精密机械与物理研究所, 吉林 长春 130033;
2. 洛阳理工学院 材料科学与工程系, 河南 洛阳 471023)

摘要: 研究了980 nm激发下 β-$NaYF_4$: Yb^{3+}, Er^{3+} 纳米片在不同温度下的上转换发光。在不同温度下,观察到了较强的绿色和红色上转换发光,分别对应于 Er^{3+} 的($^2H_{11/2}$, $^4S_{3/2}$) → $^4I_{15/2}$ 和 $^4F_{9/2}$ → $^4I_{15/2}$ 能级跃迁。随着温度的升高,520 nm 的绿色发光带和660 nm 的红色发光带强度逐渐增大,545 nm 的绿色发光带呈现出先增强(84 ~ 204 K)后减弱的趋势(204 ~ 483 K)。分析了样品上转换发光随温度变化的原因,并用三能级模型对样品的上转换发光随温度的变化规律进行了理论分析。

关 键 词: 上转换; β-$NaYF_4$; 稀土离子; 温度相关; 三能级模型

收稿日期: 2013-04-02; **修订日期**: 2013-04-18
基金项目: 国家自然科学基金(11204122,61275197); 河南省教育厅自然科学计划(12B430016)资助项目
作者简介: 赵军伟(1981 -), 男, 河南周口人, 主要从事光电子材料与器件的研究。
E-mail: jwzhao2010@lit. edu. cn

1 Introduction

Over the past decade, rare earth-doped micro-/nanocrystals with upconversion luminescence have become more prominent in photoelectric device and biological sciences due to their unique energy level structures and luminescent properties[1-7]. It is important for rare earth ions to choose appropriate host materials in order to obtain high efficient upconversion luminescent signals[8]. In recent years, fluoride micro-/nanocrystals have been paid more attention due to their relative low phonon energy, which leads to low nonradiative decay rates and high radiative emission rates for the energy levels of rare earth ions[9-10]. Therefore, strong upconversion luminescent emission can be easily observed in Er^{3+}-doped fluoride crystals, and the upconversion mechanisms have been analyzed in detail. Besides the inherent properties of the upconversion nanoparticles, the upconversion luminescence is also correlated with external factors such as the intensity of the excitation power and thermal conditions[11-12].

As we know, β-$NaYF_4$ has been regarded as one of the most effective host materials for upconversion luminescence[1,10]. Most of reports about Er^{3+}-doped β-$NaYF_4$ micro-/nanocrystals focus on synthesis, upconversion luminescence at room temperature and their applications in photoelectric device and biomedicine experiments of proofs of concept[2,13]. It is found that the intensity ratio of the two green emissions, $^2H_{11/2}\rightarrow{}^4I_{15/2}$ over $^4S_{3/2}\rightarrow{}^4I_{15/2}$, of Er^{3+} ions is an even more sensitive parameter for examining the thermal change due to the very narrow energy gap ΔE between the $^2H_{11/2}$ and $^4S_{3/2}$ levels (700 cm^{-1})[14-15]. Therefore, studying the temperature dependence of upconversion luminescence processes has been one of the key issues to explore the thermal sensitivity of Er^{3+} and Yb^{3+}/Er^{3+} codoped upconversion nanocrystals for the potential thermal sensing and biosensor materials[16-18].

However, to the best of our knowledge, there are a few of reports about the temperature dependence of upconversion luminescence processes involving Er^{3+} ions doped into β-$NaYF_4$ nanophosphors[19]. The development of cryogenic temperature equipment provides the technology for studying the optical properties of materials[20-24]. In this paper, temperature dependent novel characteristics of infrared-to-visible upconversion luminescence from β-$NaYF_4$: Yb^{3+}, Er^{3+} nanoplates were reported, and the dependence of intensity characteristics on temperature was systematically analyzed by a simple three-level system.

2 Experiments

2.1 Preparation of β-$NaYF_4$: 10% Yb^{3+}, 1% Er^{3+} Nanoplates

The β-$NaYF_4$: 10% Yb^{3+}, 1% Er^{3+} (mole fraction) nanoplates were synthesized according to our previous reports with slightly modification[25-26]. An aqueous solution of $Ln(NO_3)_3\cdot 6H_2O$ (0.1 mol/L) was mixed with an aqueous solution of trisodium citrate under vigorous stirring, and a white precipitate of lanthanide-citrate complex was formed. An aqueous solution of NaF was then added slowly into the above mixture and the pH kept at 6.5. After being stirred for 1 h, the resulting clear precursor solution was transferred to a 50 mL autoclave. The autoclave was then placed in a digital type temperature controlled oven and heated at 200 ℃ for 2 h, and then allowed to cool to room temperature naturally. After that, the precipitate of $NaYF_4$: Yb^{3+}, Er^{3+} phosphors in the autoclave could be separated from the reaction media by centrifugation (6 500 r/min, 15 min) and then washed several times with deionized water. After being dried under vacuum at 60 ℃ for 24 h, $NaYF_4$: Yb^{3+}, Er^{3+} phosphors were obtained.

2.2 Characterization

The obtained samples were characterized by X-ray powder diffractometer (XRD) using a Brucker D8-advance X-ray Diffractometer with Cu Kα radiation (λ = 0.154 18 nm), the operation voltage and current were 40 kV and 40 mA, respectively. The 2θ angle ranges from 15° to 60° in steps of 0.021° with a count time of 0.2 s. The size and morphology of $NaYF_4$: Yb^{3+}, Er^{3+} were characterized by field emission scanning electron microscopy (FESEM, Hitachi, S-4800). The upconversion emission spectra

of Er^{3+} in the β-$NaYF_4$ nanoplates were acquired using a Jobin-Yvon LabRam Raman spectrometer system equipped with a Peltier air-cooled CCD detector and 1 800 and 600 grooves/mm holographic gratings. Precise control of the sample temperature (±0.1 ℃) was achieved by means of a Linkam THMS600 temperature programmable heating/cooling microscope stage. The THMS stage was used in conjunction with a Linkam LNP cooling system when cooling. Samples were excited by a semiconductor diode laser with a 980 nm wavelength.

3 Results and Discussion

Fig. 1 shows the XRD pattern and SEM image of the β-$NaYF_4$: Yb^{3+}, Er^{3+} nanoplates. As can be seen from Fig. 1(a), the XRD peaks match well with those of standard β-$NaYF_4$ (JCPDS:28-1192). The peaks shown in the XRD pattern are sharp and intense, indicating good crystallisation of the sample[25-26]. It is observed that the obtained β-$NaYF_4$: Yb^{3+}, Er^{3+} nanoplates are uniform and monodisperse with the size of ~ 600 nm × 400 nm (side length × thickness, Fig. 1(b)).

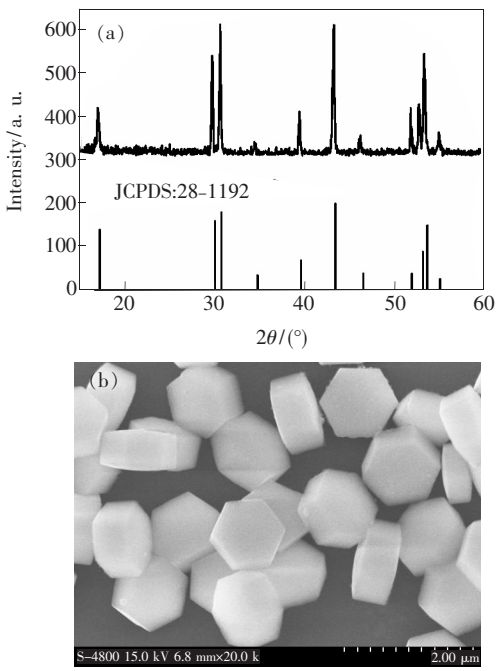

Fig. 1 XRD pattern (a) and SEM image (b) of β-$NaYF_4$: Yb^{3+}, Er^{3+} nanoplates

The upconversion process in Yb^{3+}/Er^{3+} codoped nanocrystals has been verified to be an energy transfer upconversion (ETU) involving the cross relaxation (irradiative or nonirradiative) at intermediate energy levels among Er^{3+} and Yb^{3+} ions[1,11]. The two-photon upconversion mechanism described here as follow: an Yb^{3+} ion in ground-state $^2F_{7/2}$ absorbs a photon and transits to excited-state $^2F_{5/2}$, and then the second 980 nm photon transfers the energy from an Yb^{3+} ion to populate the $^4F_{7/2}$ level of the Er^{3+} ion *via* an ETU process. This energy can then relax nonradiatively to the $^2H_{11/2}$ and $^4S_{3/2}$ levels, and the green $^2H_{11/2}\rightarrow{}^4I_{15/2}$ (525 nm) and $^4S_{3/2}\rightarrow{}^4I_{15/2}$ (545 nm) emissions occur. Alternatively, the Er^{3+} ion can further relax and populate the $^4F_{9/2}$ level, leading to the red emission of $^4F_{9/2}\rightarrow{}^4I_{15/2}$ (660 nm). Sometimes, the first absorbed phonon from Yb^{3+} ion drops back to the ground state while transferring the energy to an adjacent Er^{3+} ion, which populates the $^4I_{11/2}$ level from the ground state $^4I_{15/2}$. The energy can relax nonirradiatively to the $^4I_{13/2}$ level. The ions in this level are excited to the $^4F_{9/2}$ state *via* the energy transfer from Yb^{3+} ions.

Fig. 2(a) shows the upconversion luminescence spectra of β-$NaYF_4$: 10% Yb^{3+}, 1% Er^{3+} nanoplates excited by CW laser radiation at 980 nm at different temperatures. Fig. 2(b) is the magnification of the green emission at different temperatures. The green emission bands were observed at 525 and 545 nm and corresponding to the $^2H_{11/2}\rightarrow{}^4I_{15/2}$ and $^4S_{3/2}\rightarrow{}^4I_{15/2}$ transitions of Er^{3+} ions. The red emission bands were observed at 660 nm corresponding to the $^4F_{9/2}\rightarrow{}^4I_{15/2}$ transition of Er^{3+} ions. It is worth noting that the three upconversion emission bands are changed greatly with the temperature. At 84 K, the transition originating from the $^2H_{11/2}$ level to the ground state was not observed, while the two emission bands from the $^4S_{3/2}\rightarrow{}^4I_{15/2}$ and $^4F_{9/2}\rightarrow{}^4I_{15/2}$ transitions could be observed clearly. However, as the temperature was increased to 124 K, the $^2H_{11/2}\rightarrow{}^4I_{15/2}$ transition was just now observed, which is the well-known green hot band (Fig. 2(b)). Following the measured temperature increased from 124 to 483 K, the upconversion luminescence intensity of the $^2H_{11/2}\rightarrow{}^4I_{15/2}$ transition increased all the time (Fig. 3(a)).

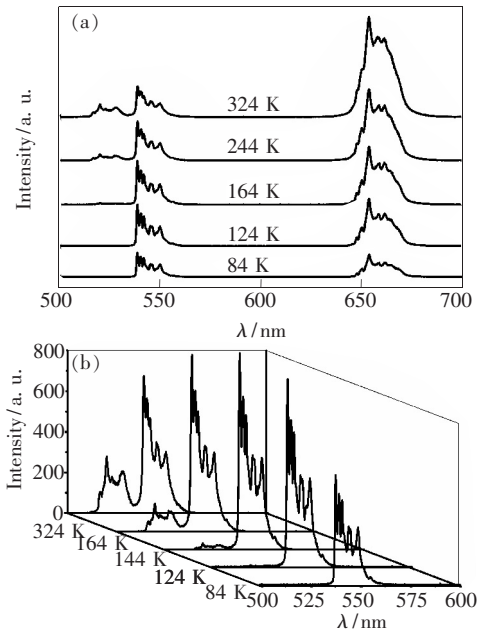

Fig. 2　(a) Upconversion luminescence spectra of β-$NaYF_4$: 10% Yb^{3+}, 1% Er^{3+} nanoplates excited by CW laser radiation at 980 nm at different temperatures. (b) The magnification of the green emission.

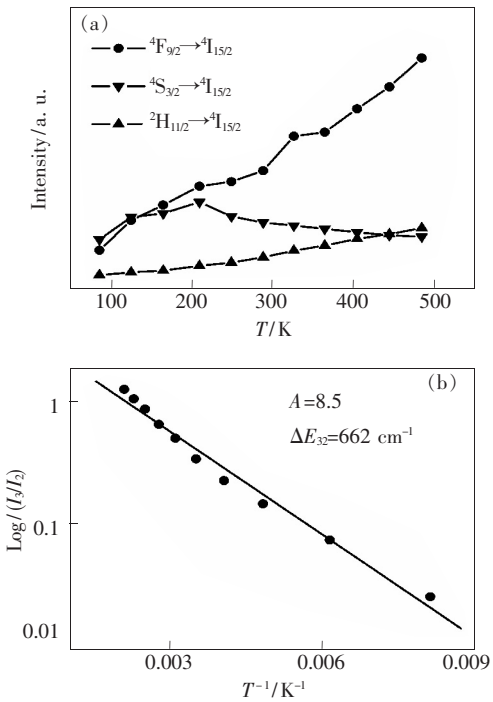

Fig. 3　(a) Green and red upconversion emission intensity as a function of temperature. (b) Logarithm of the integrated intensity ratio of the $^2H_{11/2}\rightarrow{}^4I_{15/2}$ to $^4S_{3/2}\rightarrow{}^4I_{15/2}$ transitions as a function of the absolute temperature ($1/T$).

The emission around 545 nm from the $^4S_{3/2}\rightarrow{}^4I_{15/2}$ transition increases from 84 to 204 K and reaches the largest value around 204 K, then decreases from 204 to 483 K (Fig. 3(a)). The phenomena are similar with the result of Er^{3+} doped tellurite glasses, the reasons of which are attributed to the ET mechanisms and multiphonon relaxation dependent of tempetature[24]. As we all know, the $^2H_{11/2}$ population is at the expense of the $^4S_{3/2}$ depopulation because the $^4S_{3/2}$ state is the feeding level for the $^2H_{11/2}$ level[21-23]. The more $^2H_{11/2}$ Stark levels are populated by the electrons which are produced by the thermal excitation with the increase of temperature. Interestingly, the total intensity of the red emission corresponding to the $^4F_{9/2}\rightarrow{}^4I_{15/2}$ transition increased with increasing temperature(Fig. 3(a)). This phenomenon is not observed from other upconversion nanomaterials in the previous reports[22-23]. It is found that the multiphonon relaxation rates are increased with increasing of temperature, which may influence the $^4F_{9/2}$ population[24,26].

The relative populations of the $^4S_{3/2}$ and $^2H_{11/2}$ levels can be predicted using a three-level model, which is composed of $^4I_{15/2}$ ground level (level 1), $^4S_{3/2}$ excited level (level 2) and $^2H_{11/2}$ excited level (level 3). The following equation can be used to express the thermal population of the $^2H_{11/2}$ level[20-23]:

$$\frac{I_3}{I_2} = A\exp\left(\frac{-\Delta E_{32}}{kT}\right), \qquad (1)$$

where I_3 and I_2 are the integrated upconversion emission intensities of the $^2H_{11/2}\rightarrow{}^4I_{15/2}$ and $^4S_{3/2}\rightarrow{}^4I_{15/2}$ transitions of the Er^{3+} ion, respectively, T is the absolute temperature, k is Boltzmann's constant, and ΔE_{32} is the energy gap between the $^2H_{11/2}$ and $^4S_{3/2}$ levels. The pre-exponential factor, A, is expressed by the following equation[20,22-23]:

$$A = \frac{W_{R3}g_3h\nu_3}{W_{R2}g_2h\nu_2}, \qquad (2)$$

where W_{R3} and W_{R2} are the radiative probabilities of two transitions, $h\nu_3$ and $h\nu_2$ are the photon energies of the respective transitions from levels 3 and 2 to level 1, and g_3 and g_2 are the $(2J+1)$ degeneracies of levels 3 and 2, respectively. The calculated values of $\lg(I_3/I_2)$ as a function of $1/T$ were fitted using a straight line. From the function, an energy

gap of 662 cm^{-1} was obtained (Fig. 3(b)). Compared with calculated $\Delta E_{32} = 725$ cm^{-1} from the upconversion luminescence spectra at room temperature, ΔE_{32} is a reasonable value if one neglects the Stoke's shifts caused by the temperature. It is well known that the emission intensity of $^4S_{3/2} \rightarrow {}^4I_{15/2}$ and $^4F_{9/2} \rightarrow {}^4I_{15/2}$ transitions are proportional to the population at the excited level $^4F_{7/2}$ of Er^{3+}, which is influenced by many factors, such as temperature, energy transfer mechanisms, nonradiative relaxation process[24]. The detailed study on the population at the excited levels of Er^{3+} will be present in the next work.

4 Conclusion

In summary, temperature dependent characteristics of infrared-to-visible upconversion luminescence emission in β-$NaYF_4$: 10% Yb^{3+}, 1% Er^{3+} nanoplates excited at 980 nm under cryogenic temperatures were reported. The intensity of green emission around 520 nm shows continuous increase with increasing of temperature. The emission intensity around 545 nm increases from 84 to 204 K, reaches the largest value around 204 K, and then decreases from 204 to 483 K. The intensity of red emission around 660 nm increases from 84 to 483 K. The dependence of intensity characteristics on temperature was systematically analyzed by a simple three-level system. The results presented in this study may provide useful information and new insights for further development of upconversion luminescence in micro-/nanocrystals.

References:

[1] Auzel F. Upconversion and anti-Stokes processes with f and d ions in solids [J]. *Chem. Rev.*, 2004, 104(1): 139-174.

[2] Sun C J, Xu Z H, Yan B H, *et al.* Application of $NaYF_4$: Yb, Er upconversion fluorescence nanocrystals for solution-processed near infrared photodetectors [J]. *Appl. Phys. Lett.*, 2007, 91(19): 191113-1-3.

[3] Wang F, Banerjee D, Liu Y S, *et al.* Upconversion nanoparticles in biological labeling, imaging, and therapy [J]. *Analyst.*, 2010, 135(8): 1839-1854.

[4] Wang F, Liu X G. Recent advances in the chemistry of lanthanide-doped upconversion nanocrystals [J]. *Chem. Soc. Rev.*, 2009, 38(4): 976-989.

[5] Zhou J, Zhu X J, Chen M, *et al.* Water-stable $NaLuF_4$-based upconversion nanophosphors with long-term validity for multimodal lymphatic imaging [J]. *Biomater.*, 2012, 33(26): 6201-6210.

[6] Li L L, Zhang R B, Yin L L, *et al.* Biomimetic surface engineering of lanthanide-doped upconversion nanoparticles as versatile bioprobes [J]. *Angew. Chem. Int. Ed.*, 2012, 51(25): 6121-6215.

[7] Zhou A G, Wei Y C, Wu B Y, *et al.* Pyropheophorbide *a* and *c*(RGDyK) comodified chitosan-wrapped upconversion nanoparticle for targeted near-infrared photodynamic therapy [J]. *Mol. Pharmaceutics.*, 2012, 9(6): 1580-1589.

[8] Shen J, Sun L D, Yan C H. Luminescent rare earth nanomaterials for bioprobe applications [J]. *Dalton Trans.*, 2008, 9226(42): 5687-5697.

[9] Rahman P, Green M. The synthesis of rare earth fluoride based nanoparticles [J]. *Nanoscale*, 2009, 1(2): 214-224.

[10] Li C X, Lin J. Rare earth fluoride nano-/microcrystals: Synthesis, surface modification and application [J]. *J. Mater. Chem.*, 2010, 20(33): 6831-6847.

[11] Pollnau M, Gamelin D R, Lüthi S R, *et al.* Power dependence of upconversion luminescence in lanthanide and transition-metal-ion systems [J]. *Phys. Rev.* B, 2000, 61(5): 3337-3346.

[12] Suyver J F, Aebischer A, García-Revilla S, *et al.* Anomalous power dependence of sensitized upconversion luminescence [J]. *Phys. Rev.* B, 2005, 71(12): 125123-1-9.

[13] Idris N M, Gnanasammandhan M K, Zhang J, *et al.* In vivo photodynamic therapy using upconversion nanoparticles as remote-controlled nanotransducers [J]. *Nat. Med.*, 2012, 18(10): 1580-1585.

[14] Berthou H, Jorgensen C K. Optical-fiber temperature sensor based on upconversion-excited fluorescence [J]. *Opt. Lett.*, 1990, 15(9): 1100-1102.

[15] Wade S A, Collins S F, Baxter G W. Fluorescence intensity ratio technique for optical fiber point temperature sensing

[*J*]. *J. Appl. Phys.*, 2003, 94(8):4743-4756.

[16] Wang X, Kong X G, Yu Y, *et al.* Effect of annealing on upconversion luminescence of ZnO: Er^{3+} nanocrystals and high thermal sensitivity [J]. *J. Phys. Chem.* C, 2007, 111(41):15119-15124.

[17] Bai X, Song H W, Pan G H, *et al.* Size-dependent upconversion luminescence in Er^{3+}/Yb^{3+}-codoped nanocrystalline yttria: Saturation and thermal effects [J]. *J. Phys. Chem.* C, 2007, 111(36):13611-13617.

[18] Lei Y Q, Song H W, Yang L M, *et al.* Upconversion luminescence, intensity saturation effect, and thermal effect in Gd_2O_3: Er^{3+}, Yb^{3+} nanowires [J]. *J. Chem. Phys.*, 2005, 123(17):174710-1-5.

[19] Shan J N, Kong W J, Wei R. An investigation of the thermal sensitivity and stability of the β-$NaYF_4$: Yb, Er upconversion nanophosphors [J]. *J. Appl. Phys.*, 2010, 107(5):054901-1-5.

[20] Wu X, Dai S, Toth L M, *et al.* Green upconversion emission from Er^{3+} ion doped into sol-gel silica glasses under red light (647.1 nm) excitation [J]. *J. Phys. Chem.*, 1995, 99(13):4447-4450.

[21] Vetrone F, Boyer J C, Capobianco J A. NIR to visible upconversion in nanocrystalline and bulk Lu_2O_3: Er^{3+} [J]. *J. Phys. Chem.* B, 2002, 106(22):5622-5628.

[22] Wang X, Kong X G, Shan G Y, *et al.* Luminescence spectroscopy and visible upconversion properties of Er^{3+} in ZnO nanocrystals [J]. *J. Phys. Chem.* B, 2004, 108(48):18408-18413.

[23] Sun Y J, Liu H J, Wang X, *et al.* Optical spectroscopy and visible upconversion studies of YVO_4: Er^{3+} nanocrystals synthesized by a hydrothermal process [J]. *Chem. Mater.*, 2006, 18(11):2726-2732.

[24] Shen X, Nie Q H, Xu T F, *et al.* Temperature dependence of upconversion luminescence in erbium-doped tellurite glasses [J]. *J. Lumin.*, 2010, 130(8):1353-1356.

[25] Sun Y J, Chen Y, Tian L J, *et al.* Controlled synthesis and morphology dependent upconversion luminescence of $NaYF_4$: Yb, Er nanocrystals [J]. *Nanotechnol.*, 2007, 18(27):275609-1-9.

[26] Zhao J W, Sun Y J, Kong X G, *et al.* Controlled synthesis, formation mechanism, and great enhancement of red upconversion luminescence of $NaYF_4$: Yb^{3+}, Er^{3+} nanocrystals/nanoplates at low doping level [J]. *J. Phys. Chem.* B, 2008, 112(49):15666-15672.